IOP Conference Series: Materials Science and Engineering

PAPER • **OPEN ACCESS**

Vibration Suppression of a Cantilevered Piezoelectric Laminated Composite Plate Subjected to Hygrothermal Loads

To cite this article: Yue Jiang *et al* 2019 *IOP Conf. Ser.: Mater. Sci. Eng.* **531** 012035

IOP Conf. Series: Materials Science and Engineering **531** (2019) 012035 doi:10.1088/1757-899X/531/1/012035

Vibration Suppression of a Cantilevered Piezoelectric Laminated Composite Plate Subjected to Hygrothermal Loads

Yue Jiang, Ning Xue, Shufeng Lu, Xiaojuan Song

Department of Mechanics, Inner Mongolia University of Technology, Hohhot 010051, P. R. China

E-mail: shufenglu@163.com

Abstract. In this paper, the vibration suppression strategy for a cantilevered rectangular piezoelectric laminated composite plate is proposed by using the piezoelectric patches, which are attached to the upper and lower surfaces of the plate as the actuators and sensors, respectively. The main contributions of this study is as follows: Firstly, Based on classical laminated plate theory and considering the action of piezoelectric loadings, the dynamics equation of a piezoelectric laminated composite plate subjected to hygrothermal loads is derived by using Hamilton's principle. The partial differential equations of the piezoelectric laminated composite plate are discretized to a two-degree-of-freedom control equation by using Galerkin method. Secondly, According to the discrete nominal model, a robust controller for the uncertain systems is proposed. Based on the state space equation, the output feedback controller for the system is designed. In the constructed full-dimensional state observer, the estimated state feedback is introduced to construct a closed-loop feedback system. Using the Lyapunov Matrix Inequality (LMI) method and Lyapunov Stability Theory, the feedback gain matrix and observation gain matrix for the system are designed to make the closed-loop system asymptotically stable. Finally, the accuracy and effectiveness of the controller are verified by numerical simulation.

1. Introduction

Recently, piezoelectric materials as a new smart material have been widely used as actuators and sensors embedded in engineering structures to form a piezoelectric composite structure to improve the controllability. Piezoelectric composite structure is widely used in spacecraft, large space station and other engineering fields [1-4]. Therefore, it is of great theoretical and engineering application value to study the vibration suppression of piezoelectric laminated composite plate subjected to hygrothermal loads.

Vibration of composite structures subjected to the hygrothermal loads has raised a large interest. Some scholars solved the vibration problem under hygrothermal stress by the way of the finite element formula. The core idea of Sreehari et al. [5] is to analyze the buckling analysis of laminated composite plate the subjected to the in-plane thermal and moisture loads by using code in the Matlab environment. Ram et al. [6] modified on the traditional finite element method and proposed the effect of temperature and humidity on the free vibration of laminated composite plate Radic et al. [7] established an equation to study the vibrational behaviour of the nano-plates embedded with grapheme patches under the in-plane hygrothermal loads and the analysis of the critical buckling load was presented under the seven different boundary systems.

Some scholars assumed the material parameter as a function of the temperature and moisture in the case of the hygrothermal stress problem of the functionally graded plates. Malekzadeh et al. [8] investigated the free vibration of a functionally graded straight-sided quadrilateral plate in a thermal environment and the material properties of the plate depend on the temperature. Mahapatraa et al. [9] considered that the material properties are the function about the temperature and moisture concentration. The nonlinear free vibrational natural frequency of the laminated composite spherical shell panel subjected to the in-plane thermal and humidity loading is studied. Rath et al. [10] analyzed the free vibration of composite laminates in different temperatures and moisture concentration by conducted experimental and numerical studies. Shenas et al. [11] studied the effects of thermal environment and geometric parameters to the free vibrational behaviour of functionally graded (FG) quadrilateral micro-plates. Ye et al. [12] studied the hygrothermal vibration behaviour of multi-layered cylindrical shells by the way of the 3-D elasticity theory under general boundary conditions.

Vibration usually causes damage to the engineering structure. Thus, it is essential to study the vibration suppression. Phung-Van et al. [13] proposed the vibration suppression and the control of the static deflection for the isotropic Mindlin plates via the displacement and velocity feedback controller. And the cell-based smoothed discrete shear gap method (CS-FEM-DSG3) was used to analyse the free vibration behaviour. He et al. [14] proposed a finite element formula for vibration suppression of functionally graded material structure based on classical laminate theory and designed the constant velocity feedback controller to damp out the vibration behaviour of the FGM plates. Song et al. [15] designed a controller by the way of velocity feedback control strategy and studied the influence of the location of the piezoelectric patches on the vibration control of the carbon nanotube (CNT) reinforced functionally graded plates.

Most of the previous investigations of vibration suppression are about simply supported composite laminates. Moreover, few researchers have conducted the active vibration suppression of composite cantilever plates in the hygrothermal environment. In this paper, the free vibrational response and vibration suppression for a cantilevered rectangular piezoelectric laminated composite plate under the hygrothermal loading are proposed. Governing equation is formulated by Classical Laminated Plate Theory, Hamilton's principle and Galerkin method. A robust controller for the uncertain systems is presented via the discrete nominal model. The influences of the temperature and moisture concentration on free vibration behaviour of the cantilevered rectangular piezoelectric laminated composite plate are calculated. In addition, the effectiveness and accuracy of the vibration controller are proposed.

2. Establishment of dynamics Equation

The mechanical model of the piezoelectric composite cantilever laminated plate is shown in Figure 1. The length of the plate is a, the width is b, the plate is placed in a hygrothermal environment. A coordinate system $Oxyz$ is placed in the mid-plane of the piezoelectric laminated composite rectangular cantilever plate. In addition, the thickness of the plate is average and equal to h, the number of layer is k, the layer angle is θ. Piezoelectric actuators and sensors with the same thickness t_p are placed on top and bottom of the laminate, respectively.

In view of the classical laminated plate theory [16, 17], the displacement fields are described as follows

$$u(x,y,t) = u_0(x,y,t) - z\frac{\partial w_0}{\partial x} \tag{1-a}$$

$$v(x,y,t) = v_0(x,y,t) - z\frac{\partial w_0}{\partial y} \tag{1-b}$$

$$w(x,y,t) = w_0(x,y,t) \tag{1-c}$$

where u_0, v_0 and w_0 are the displacements components of any point along the coordinate x, y and z direction on the mid-plane. The Geometric equation can be described as

$$\varepsilon_{xx} = \frac{\partial u}{\partial x},\ \varepsilon_{yy} = \frac{\partial v}{\partial y},\ \varepsilon_{xy} = \frac{1}{2}(\frac{\partial u}{\partial y} + \frac{\partial v}{\partial x}) \tag{2}$$

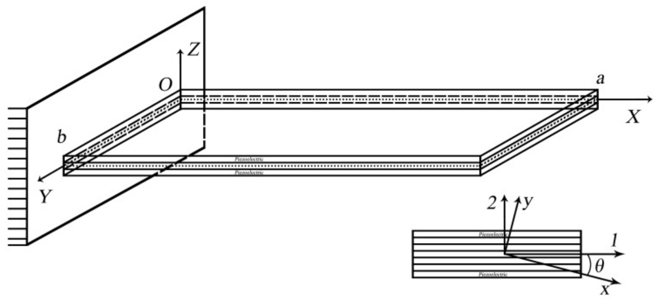

Figure 1. The model of cantilevered piezoelectric laminated composite plate and the coordinate system

Considering the temperature change and moisture environment, the constitutive equation of the *k-th* orthotropic lamina in the principal material coordinate direction is

$$\begin{bmatrix} \sigma_1 \\ \sigma_2 \\ \sigma_6 \end{bmatrix}^{(k)} = \begin{bmatrix} Q_{11} & Q_{12} & 0 \\ Q_{12} & Q_{22} & 0 \\ 0 & 0 & Q_{66} \end{bmatrix}^{(k)} \begin{bmatrix} \varepsilon_1 - \alpha_1 \Delta T - \beta_1 C \\ \varepsilon_2 - \alpha_2 \Delta T - \beta_2 C \\ \gamma_6 \end{bmatrix}^{(k)} \tag{3}$$

where α_1, α_2 are the coefficient of thermal expansion along x_1 and x_2, β_1 and β_2 are the moisture expansion coefficient along x_1 and x_2, ΔT=T-T$_0$ is the temperature increment for an orthotropic composite single layer without external load, $C = \frac{\Delta M}{M}$ is the concentration of water absorbed by orthotropic laminated composite plate in a moisture environment, and the coefficients $Q_{ij}^{(k)}(i, j = 1,2,6)$ are the engineering elastic constants of the *k-th* layer and are described by

$$Q_{11} = \frac{E_1}{1 - \upsilon_{12}\upsilon_{21}},\ Q_{22} = \frac{E_2}{1 - \upsilon_{12}\upsilon_{21}},\ Q_{12} = Q_{21} = \frac{\upsilon_{21}E_1}{1 - \upsilon_{12}\upsilon_{21}} = \frac{\upsilon_{12}E_1}{1 - \upsilon_{12}\upsilon_{21}},\ Q_{66} = G_{66} \tag{4}$$

Since the laminates are composed of some orthotropic layers, which the materials are oriented randomly with respect to the plate coordinates. Thus, the stress-strain relations of each layer must use the unified coordinate system $Oxyz$, that is [18, 19]

$$\begin{bmatrix} \sigma_{xx} \\ \sigma_{yy} \\ \sigma_{xy} \end{bmatrix}^{(k)} = \begin{bmatrix} \overline{Q}_{11} & \overline{Q}_{12} & \overline{Q}_{16} \\ \overline{Q}_{12} & \overline{Q}_{22} & \overline{Q}_{26} \\ \overline{Q}_{16} & \overline{Q}_{26} & \overline{Q}_{66} \end{bmatrix}^{(k)} \begin{bmatrix} \varepsilon_{xx} - \alpha_{xx}\Delta T - \beta_{xx} C \\ \varepsilon_{yy} - \alpha_{yy}\Delta T - \beta_{yy} C \\ \gamma_{xy} - \alpha_{xy}\Delta T - \beta_{xy} C \end{bmatrix}^{(k)} \tag{5}$$

where $\overline{Q}_{ij}(i, j = 1,2,6)$ is the transformation matrix of stiffness matrix Q of the principal material coordinate direction, α_{xx}, α_{yy} and α_{xy} are the thermal coefficients of expansion which has been transformed, and the transformation relations are written as

$$\alpha_{xx} = \alpha_1 \cos^2\theta + \alpha_2 \sin^2\theta,\ \alpha_{yy} = \alpha_1 \sin^2\theta + \alpha_2 \cos^2\theta,\ \alpha_{xy} = 2(\alpha_1 - \alpha_2)\sin\theta\cos\theta \tag{6a}$$

where β_{xx}, β_{yy} and β_{xy} are the moisture expansion coefficient under the *x-y* coordinate system, and the transformation relations are written as

$$\beta_{xx} = \beta_1 \cos^2\theta + \beta_2 \sin^2\theta,\ \beta_{yy} = \beta_1 \sin^2\theta + \beta_2 \cos^2\theta,\ \beta_{xy} = 2(\beta_1 - \beta_2)\sin\theta\cos\theta \tag{6b}$$

Using the Hamilton principle, the governing equations can be obtained as follows [16]

$$\int_{t_1}^{t_2} (\delta K - \delta U)dt + \int_{t_1}^{t_2} \delta W dt = 0 \tag{7}$$

where δK , δU and δW represents the kinetic energy, the strain energy and the virtual work respectively.

The virtual work is generated by the piezoelectric actuator at the input voltage $V_a(x, y, t)$ due to the ignored of effects of damping and is given by [20]

$$\delta W = \iint V_a(x, y, t)\delta D_3^{ap}(x, y, t)dxdy \tag{8}$$

where $D_3^{ap}(x, y, t)$ is the electro-displacement field along the z-axis for actuator patch.

Here, the composite laminates are alternated composed of orthotropic single-layer plates with the angle between the principal material direction and the coordinate axis being 0° and 90°.

Using equations (7) and (8), the kinetic equation is obtained by using the variational method. Also, the δD_3^{ap} and δD_3^{sp} (in the δu_0 , δv_0 , δw_0 equation) are replaced by using the electric displacement fields D_3^{ap} and D_3^{sp} . Thus, the vibration differential equation of the laminated composite thin plate with piezoelectric actuator and sensor express as follows [5, 9, 21]

δu_0 :

$$\begin{aligned} &I_0\ddot{u}_0 - I_1\frac{\partial \ddot{w}_0}{\partial x} - (A_{11} + 2A_{11}^{ap})\frac{\partial^2 u_0}{\partial x^2} - (A_{12} + 2A_{12}^{ap})\frac{\partial^2 v_0}{\partial x \partial y} - A_{66}(\frac{\partial^2 u_0}{\partial y^2} + \frac{\partial^2 v_0}{\partial x \partial y}) \\ &+2\frac{h_{31}^{a\,2}}{\beta_{33}^{ap}}(\frac{\partial^2 u_0}{\partial x^2} + \frac{\partial^2 v_0}{\partial x \partial y}) - \frac{h_{31}^{a}}{\beta_{33}^{ap}}\frac{\partial V_a(x, y, t)}{\partial x} = 0 \end{aligned} \tag{9}$$

δv_0 :

$$\begin{aligned} &I_0\ddot{v}_0 - I_1\frac{\partial \ddot{w}_0}{\partial y} - (A_{12} + 2A_{12}^{ap})\frac{\partial^2 u_0}{\partial x \partial y} - (A_{22} + 2A_{22}^{ap})\frac{\partial^2 v_0}{\partial y^2} - A_{66}(\frac{\partial^2 u_0}{\partial x \partial y} + \frac{\partial^2 v_0}{\partial x^2}) \\ &+2\frac{h_{31}^{a\,2}}{\beta_{33}^{ap}}(\frac{\partial^2 v_0}{\partial y^2} + \frac{\partial^2 u_0}{\partial x \partial y}) - \frac{h_{31}^{a}}{\beta_{33}^{ap}}\frac{\partial V_a(x, y, t)}{\partial y} = 0 \end{aligned} \tag{10}$$

δw_0 :

$$\begin{aligned} &I_0\ddot{w}_0 + D_{11}\frac{\partial^4 w_0}{\partial x^4} + 2D_{12}\frac{\partial^4 w_0}{\partial x^2 \partial y^2} + D_{22}\frac{\partial^4 w_0}{\partial y^4} + 4D_{66}\frac{\partial^4 w_0}{\partial x^2 \partial y^2} + D_{11}^{ap}\frac{\partial^4 w_0}{\partial x^4} + 2D_{12}^{ap}\frac{\partial^4 w_0}{\partial x^2 \partial y^2} + D_{22}^{ap}\frac{\partial^4 w_0}{\partial y^4} \\ &D_{11}^{sp}\frac{\partial^4 w_0}{\partial x^4} + 2D_{12}^{sp}\frac{\partial^4 w_0}{\partial x^2 \partial y^2} + D_{22}^{sp}\frac{\partial^4 w_0}{\partial y^4} - (\frac{h_{31}^{ap2}}{\beta_{33}^{ap}} + \frac{h_{31}^{sp2}}{\beta_{33}^{ap}})(\frac{\partial^4 w_0}{\partial x^4} + 2\frac{\partial^4 w_0}{\partial x^2 \partial y^2} + \frac{\partial^4 w_0}{\partial y^4}) + \frac{h_{31}^{ap}}{\beta_{33}^{ap}}(\frac{\partial^2 V_a}{\partial x^2} + \frac{\partial^2 V_a}{\partial y^2}) \\ &-(N_a^T + N_s^T)(\frac{\partial^2 w_0}{\partial x^2} + \frac{\partial^2 w_0}{\partial y^2}) + \Delta T((A_{11}^T + A_{12}^T + A_{16}^T)\frac{\partial^2 w_0}{\partial x^2} + (B_{12}^T + B_{22}^T + B_{26}^T)\frac{\partial^2 w_0}{\partial y^2} \\ &+4(D_{16}^T + D_{26}^T + D_{66}^T)\frac{\partial^2 w_0}{\partial x \partial y}) + C((A_{11}^C + A_{12}^C + A_{16}^C)\frac{\partial^2 w_0}{\partial x^2} + (B_{12}^C + B_{22}^C + B_{26}^C)\frac{\partial^2 w_0}{\partial y^2} + 4(D_{16}^C + D_{26}^C + D_{66}^C)\frac{\partial^2 w_0}{\partial x \partial y})) \\ &= I_2\frac{\partial^2 \ddot{w}_0}{\partial x^2} + I_2\frac{\partial^2 \ddot{w}_0}{\partial y^2} - I_1\frac{\partial \ddot{u}_0}{\partial x} - I_1\frac{\partial \ddot{v}_0}{\partial y} \end{aligned} \tag{11}$$

where,

$$(A_{ij}, B_{ij}, D_{ij}) = \sum_{k=1}^{N}\int_{z_{k-1}}^{z_k} \overline{Q}_{ij}^k(1, z, z^2)dz \;\; (i, j = 1, 2, 6) \tag{12}$$

$$(A_{ij}^T, B_{ij}^T, D_{ij}^T) = \sum_{k=1}^{N}\int_{z_{k-1}}^{z_k} \overline{Q}_{ij}^k(\alpha_{xx}^k, \alpha_{yy}^k, \alpha_{xy}^k)dz \;\; (i, j = 1, 2, 6) \tag{13}$$

$$(A_{ij}^{C}, B_{ij}^{C}, D_{ij}^{C}) = \sum_{k=1}^{N} \int_{z_{k-1}}^{z_k} \overline{Q}_{ij}^{k} (\beta_{xx}^{k}, \beta_{yy}^{k}, \beta_{xy}^{k}) dz \ (i, j = 1, 2, 6) \tag{14}$$

$$N_a^T = -\int_{\frac{h}{2}}^{\frac{h}{2}+t_p} E_p (1-\upsilon_p)^{-1} \alpha_p \Delta T dz \tag{15}$$

$$N_s^T = -\int_{-\frac{h}{2}-t_p}^{-\frac{h}{2}} E_p (1-\upsilon_p)^{-1} \alpha_p \Delta T dz \tag{16}$$

Also, $I_i = Iz^i \ (i = 0,1,2)$, $(A_{ij}^{ap}, B_{ij}^{ap}, D_{ij}^{ap}) = \int_{\frac{h}{2}}^{\frac{h}{2}+t_p} C_{ij}^{p} (1, z, z^2)\, dz \ (i, j = 1, 2)$, $(h_{31}^{a}, h_{31}^{ap}) = \int_{\frac{h}{2}}^{\frac{h}{2}+t_p} h_{31} (1, z)\, dz$, $\beta_{33}^{ap} = \int_{\frac{h}{2}}^{\frac{h}{2}+t_p} \beta_{33}^{a}\, dz$, $(A_{ij}^{sp}, B_{ij}^{sp}, D_{ij}^{sp}) = \int_{-\frac{h}{2}-t_p}^{-\frac{h}{2}} C_{ij}^{p} (1, z, z^2)\, dz \ (i, j = 1, 2)$, $(h_{31}^{s}, h_{31}^{sp}) = \int_{-\frac{h}{2}-t_p}^{-\frac{h}{2}} h_{31} (1, z)\, dz$, $\beta_{33}^{sp} = \int_{-\frac{h}{2}-t_p}^{-\frac{h}{2}} \beta_{33}^{s}\, dz$.

where, $C_{11}^{p} = C_{22}^{p} = \dfrac{E_p}{1-\upsilon_P^2}$, $C_{12}^{p} = C_{21}^{p} = \dfrac{\upsilon_P E_p}{1-\upsilon_P^2}$, $C_{16}^{p} = C_{26}^{p} = 0$, $h_{31} = h_{32}$, $h_{36} = 0$ and $\beta_{33}^{a} = \beta_{33}^{s}$. Further, E_p, υ_P, $h_{3j} (j = 1,2,6)$, D_3^{ap}, D_3^{sp}, $\beta_{33}^{i} (i = a, s)$ and α_p are the modulus of elasticity, Poisson's ratio, piezoelectric constant, the electric displacement field of the actuator, the electric displacement field of the sensor, the impermittivity constants, and the piezoelectric material's coefficient of thermal expansion (see Table 2). The superscripts *ap* and *sp* represent actuators and sensors made of piezoelectric patches, respectively.

Table 1. Typical data for Graphite/Epoxy [10, 18].

Parameter	Value	Unit
E_1	185	GPa
E_2	10.5	GPa
α_1	-0.3×10^{-6}	K^{-1}
α_2	28.1×10^{-6}	K^{-1}
β_1	0	--
β_2	0.44	--
G_{12}	7.3	GPa
υ_{12}	0.28	--
ρ	1600	$kg \cdot m^{-3}$

Table 2. Physical properties of the piezoelectric actuator/sensor (for G_1195N [14, 24, 25])

Parameter	Value	Unit
E_p	63×10^{9}	$N \cdot m^{-2}$
ρ_p	7600	$kg \cdot m^{-3}$
υ_p	0.3	--
$d_{31} = d_{32}$	254×10^{-12}	$m \cdot V^{-1}$
d_{36}	0	$m \cdot V^{-1}$
$h_{31} = h_{32}$	-39.37×10^{8}	$V \cdot m^{-1}$
β_{33}	6.667×10^{7}	$m \cdot F^{-1}$
α_p	12×10^{-4}	K^{-1}
k_p	0.17	$W \cdot (mk)^{-1}$

3. Galerkin's method

This paper mainly studies the transversal vibration for the piezoelectric laminated composite rectangular cantilever plate, ignoring the in-plane vibration (in u_0 and v_0 directions) and the coupling term in the dynamic equation. Here, the variables and parameters are introduced as follows:

$$\overline{w}=\frac{w_0}{h}\ ,\ \overline{x}=\frac{x}{a}\ ,\ \overline{y}=\frac{y}{b}\ ,\ \overline{t}=t\pi^2(\frac{E}{ab\rho})^{1/2}\ ,\ \overline{A_{ij}}=\frac{(ab)^{1/2}}{Eh^2}A_{ij}\ ,\ \lambda=\frac{a}{b}\ ,\ \beta=\frac{h}{a}\ ,\ \overline{B_{ij}}=\frac{(ab)^{1/2}}{Eh^3}B_{ij}\ ,$$

$$\overline{D_{ij}}=\frac{(ab)^{1/2}}{Eh^4}D_{ij}\ ,\ \overline{I_i}=\frac{1}{(ab)^{(i+1)/2}\rho}I_i\ ,\ \overline{A_{ij}^T}=\frac{(ab)^{1/2}}{Eh^2}A_{ij}^T\ ,\ \overline{B_{ij}^T}=\frac{(ab)^{1/2}}{Eh^2}B_{ij}^T\ ,\ \overline{D_{ij}^T}=\frac{(ab)^{1/2}}{Eh^2}D_{ij}^T$$

$$\overline{D_{ij}^{ap}}=\frac{(ab)^{1/2}}{Eh^4}D_{ij}^{ap}\ ,\ \overline{D_{ij}^{sp}}=\frac{(ab)^{1/2}}{Eh^4}D_{ij}^{sp}\ ,\ \overline{N_a^T}=\frac{(ab)^{1/2}}{Eh^2}N_a^T\ ,\ \overline{N_s^T}=\frac{(ab)^{1/2}}{Eh^2}N_s^T \tag{17}$$

The first two modes of the transverse displacement w_0 of the laminated composite cantilever rectangular plate are considered, we choose the appropriate mode function. Therefore, the transverse displacement w_0 with the first two modes is expressed as follows: [22-23]

$$w_0=w_1(t)X_1(x)Y_1(y)+w_2(t)X_2(x)Y_2(y) \tag{18}$$

where,

$$X_1(x)=\sin\frac{\lambda_1}{a}x-\sinh\frac{\lambda_1}{a}x+\alpha_1(\cosh\frac{\lambda_1}{a}x-\cos\frac{\lambda_1}{a}x) \tag{18a}$$

$$X_2(x)=\sin\frac{\lambda_2}{a}x-\sinh\frac{\lambda_2}{a}x+\alpha_2(\cosh\frac{\lambda_2}{a}x-\cos\frac{\lambda_2}{a}x) \tag{18b}$$

$$Y_1(y)=\sin\frac{\mu_1}{b}y+\sinh\frac{\mu_1}{b}y-\beta_1(\cosh\frac{\mu_1}{b}y+\cos\frac{\mu_1}{b}y) \tag{18c}$$

$$Y_2(y)=\sin\frac{\mu_2}{b}y+\sinh\frac{\mu_2}{b}y-\beta_2(\cosh\frac{\mu_2}{b}y+\cos\frac{\mu_2}{b}y) \tag{18d}$$

where $\lambda_i,\mu_j,\alpha_i,\beta_j\ \ (i,j=1,2)$ can be obtained from the following equations

$$\cos\lambda_i a\cos\lambda_i a+1=0\,,\ \cos\mu_j b\cos\mu_j b-1=0 \tag{19a}$$

$$\alpha_i=\frac{\sinh\lambda_i a+\sin\lambda_i a}{\cosh\lambda_i a+\cos\lambda_i a}\,,\ \beta_j=\frac{\sinh\mu_j b-\sin\mu_j b}{\cosh\mu_j b-\cos\mu_j b} \tag{19b}$$

where $w_1(t)$ and $w_2(t)$ represents the amplitude for the first two-order modes.

The ordinary differential equation is obtained, and the Equation (11) is discretized by the Galerkin method and the following equation is obtained

$$[\boldsymbol{M}][\ddot{\boldsymbol{w}}]+[\boldsymbol{K}][\boldsymbol{w}]=[\boldsymbol{F}]V_a \tag{20}$$

where,

$$[\boldsymbol{M}]=\begin{bmatrix} m_1 & 0\\ 0 & m_2\end{bmatrix},\ [\boldsymbol{w}]=\begin{bmatrix} w_1\\ w_2\end{bmatrix},\ [\boldsymbol{K}]=\begin{bmatrix} K_1 & K_2\\ K_3 & K_4\end{bmatrix},\ [\boldsymbol{F}]=\begin{bmatrix} F_1\\ F_2\end{bmatrix} \tag{21}$$

where, $[\boldsymbol{M}]$ and $[\boldsymbol{K}]$ are the mass and stiffness matrices, $[\boldsymbol{F}]$ is the force matrix.

Defining the state vector $\boldsymbol{X}=\begin{bmatrix} w_1 & w_2 & \dot{w}_1 & \dot{w}_2\end{bmatrix}^T$ and the elements in $\boldsymbol{X}$ are the displacement and the velocity of the mode, and the state equation (20) can be transformed into the follows

$$\dot{\boldsymbol{X}}=[\boldsymbol{A}]\boldsymbol{X}+[\boldsymbol{B}]V_a(t) \tag{22}$$

where,

$$[\boldsymbol{A}]=\begin{bmatrix} [\boldsymbol{0}] & [\boldsymbol{I}]\\ -[\boldsymbol{M}]^{-1}[\boldsymbol{K}] & [\boldsymbol{0}]\end{bmatrix},\ [\boldsymbol{B}]=\begin{bmatrix} [\boldsymbol{0}]\\ [\boldsymbol{M}]^{-1}[\boldsymbol{F}]\end{bmatrix}$$

The dynamic equation of the piezoelectric sensor is as follows [20]

$$Y = -\frac{h_{31}^{ap}}{\beta_{33}^{ap} h}\int_0^1\int_0^1 (\lambda \frac{\partial^2 w_0}{\partial x^2} + \frac{\partial^2 w_0}{\partial y^2}\lambda^{-1})\, dxdy \tag{23}$$

thus,

$$\boldsymbol{Y} = [\boldsymbol{C}]\boldsymbol{X} + [\boldsymbol{D}]V_a(t) \tag{24}$$

where $\boldsymbol{D} = 0$, $[\boldsymbol{C}] = [C_1 \quad C_2 \quad [\boldsymbol{0}]]$.

4. Designing of control method

In this part, the design of vibration controller for a laminated composite cantilever plate with piezoelectric patches is concerned. By considering the parameter uncertainties of dynamic model, Equation (22) and (24) can be described as

$$\dot{\boldsymbol{X}} = [\boldsymbol{A} + \boldsymbol{\Delta A}]\boldsymbol{X} + [\boldsymbol{B} + \boldsymbol{\Delta B}]V_a(t) \tag{25}$$

$$\boldsymbol{Y} = [\boldsymbol{C}]\boldsymbol{X} \tag{26}$$

where,

$$[\boldsymbol{\Delta A} \quad \boldsymbol{\Delta B}] = \boldsymbol{MF}[\boldsymbol{E_1} \quad \boldsymbol{E_2}] \tag{27}$$

Here, $\boldsymbol{M}$, $\boldsymbol{E_1}$ and $\boldsymbol{E_2}$ are the known constant matrix of suitable dimensions, and $\boldsymbol{F(t)}$ is time-varying matrix function and satisfies the conditions

$$\boldsymbol{F(t)^T F(t)} \leq \boldsymbol{I} \tag{28}$$

To overcome the parameter uncertainty, a robust controller is designed. By assuming that the state vector $\boldsymbol{X(t)}$ is measurable, the state feedback controller is as follows.

$$V_a(t) = -\boldsymbol{K^a X(t)} \tag{29}$$

where $\boldsymbol{K^a}$ is the feedback gain matrix of the robust controller (for detail calculation, see **Theorem 1**).

In Section 2, the piezoelectric sensor attached to the laminated composite cantilever plate, only actuator's tip displacement is measurable. This problem limits the use of the current controller [20]. In order to effectively overcome this problem, we add a full-dimensional state observer to the close loop system, which can estimate the value of $\boldsymbol{X(t)}$. The full-dimensional state observer is given by

$$\dot{\boldsymbol{X}}\boldsymbol{(t)^o} = [\boldsymbol{A}]\boldsymbol{X(t)^o} + [\boldsymbol{L}][\boldsymbol{Y} - \boldsymbol{CX(t)^o}] + [\boldsymbol{B}]V_a(t) \tag{30}$$

where, $\boldsymbol{X(t)^o}$ is the state vector which has been observed, $\boldsymbol{L}$ is the observer gain matrix. Thus, the input of the control system is transformed as

$$V_a(t) = -\boldsymbol{K^a X(t)^o} \tag{31}$$

There, we define the state observation error $\boldsymbol{e} = \boldsymbol{X(t)} - \boldsymbol{X(t)^o}$ and using formula (31) and (25), the closed-loop system can be written as

$$\dot{\boldsymbol{X}}\boldsymbol{(t)} = [\boldsymbol{A} + \boldsymbol{\Delta A} - \boldsymbol{(B + \Delta B)K^a}]\boldsymbol{X(t)} + [\boldsymbol{B} + \boldsymbol{\Delta B}]\boldsymbol{K^a e} \tag{32}$$

$$\dot{\boldsymbol{e}} = [\boldsymbol{A} - \boldsymbol{LC} + \boldsymbol{\Delta BK^a}]\boldsymbol{e} + [\boldsymbol{\Delta A} - \boldsymbol{\Delta BK^a}]\boldsymbol{X(t)} \tag{33}$$

As a result, the formula (32)-(33) are equivalent with that of formula (25)-(31).

Lemma 1 For a constant matrix of appropriate dimensions $\boldsymbol{X}$, $\boldsymbol{Y}$, for any ε >0, the following inequality is established [26]

$$\boldsymbol{X^T Y} + \boldsymbol{Y^T X} \leq \varepsilon \boldsymbol{X^T X} + \frac{1}{\varepsilon}\boldsymbol{Y^T Y} \tag{34}$$

Theorem 1 If the matrices $\boldsymbol{M}_i$ $(i = 1,2,3)$, $\boldsymbol{N}_i$ $(i = 1,2,3)$, $\boldsymbol{N}$, $\boldsymbol{T}$, and positive scalars ε_i $(i = 1,2,...5)$ which satisfied the following matrix inequality existed, the designed closed loop control system above is asymptotic stability

$$\begin{bmatrix} \boldsymbol{M}_1 & \boldsymbol{M}_2 & \boldsymbol{M}_3 \\ \boldsymbol{M}_2^T & (-\frac{1}{\varepsilon_3+\varepsilon_5})\boldsymbol{I} & 0 \\ \boldsymbol{M}_3^T & 0 & (-\frac{1}{\varepsilon_3^{-1}+\varepsilon_2^{-1}})\boldsymbol{I} \end{bmatrix} < 0 \tag{35}$$

$$\begin{bmatrix} \boldsymbol{N}_1 & \boldsymbol{N}_2 & \boldsymbol{N}_3 \\ \boldsymbol{N}_2^T & -(\varepsilon_1+\varepsilon_2)^{-1}\boldsymbol{I} & 0 \\ \boldsymbol{N}_3^T & 0 & (-\frac{1}{\varepsilon_1^{-1}+\varepsilon_5^{-1}})\boldsymbol{I} \end{bmatrix} < 0 \tag{36}$$

where,

$$\boldsymbol{N} = \boldsymbol{K}^a \boldsymbol{P}^{-1},\ \boldsymbol{M}_1 = \boldsymbol{A}\boldsymbol{P}^{-1} + \boldsymbol{P}^{-1}\boldsymbol{A}^T - \boldsymbol{B}\boldsymbol{N} - \boldsymbol{N}^T\boldsymbol{B}^T + \varepsilon_4 \boldsymbol{B}\boldsymbol{B}^T,\ \boldsymbol{M}_2 = \boldsymbol{M},\ \boldsymbol{M}_3 = \boldsymbol{P}^{-1}\boldsymbol{E}_1^T - \boldsymbol{N}^T\boldsymbol{E}_2^T \tag{37}$$

$$\boldsymbol{T} = \boldsymbol{Q}\boldsymbol{L},\ \boldsymbol{N}_1 = \boldsymbol{Q}\boldsymbol{A} + \boldsymbol{A}^T\boldsymbol{Q} - \boldsymbol{T}\boldsymbol{C} - \boldsymbol{C}^T\boldsymbol{T}^T + \varepsilon_4^{-1}\boldsymbol{K}^{aT}\boldsymbol{K}^a,\ \boldsymbol{N}_2 = \boldsymbol{Q}\boldsymbol{M},\ \boldsymbol{N}_3 = \boldsymbol{K}^{aT}\boldsymbol{E}_2^T \tag{38}$$

Let $\boldsymbol{S} = \boldsymbol{P}^{-1}$, $\boldsymbol{K}^a = \boldsymbol{N}\boldsymbol{S}$ and use Linear Matrix Inequality (LMI) to obtain $\boldsymbol{P}$ and the feedback gain matrix $\boldsymbol{K}^a$ in equation (35). Substituting $\boldsymbol{P}$ and $\boldsymbol{K}^a$ obtained by inequality (35) into inequality (36), and $\boldsymbol{L} = \boldsymbol{Q}^{-1}\boldsymbol{T}$, then, the observation gain matrix $\boldsymbol{L}$ is obtained.

The proof process of **Theorem 1** is given by

Proof 1 Considering the asymptotic stability of closed-loop systems, the Lyapunov's Direct Method is used, the scalar function is constructed as follows

$$\boldsymbol{V} = \boldsymbol{e}^T\boldsymbol{Q}\boldsymbol{e} + \boldsymbol{X}^T\boldsymbol{P}\boldsymbol{X} \tag{39}$$

where, $\boldsymbol{P}$ and $\boldsymbol{Q}$ are the symmetric positive definite matrix. In the case of $\boldsymbol{e}(\boldsymbol{t}) \neq 0$ and $\boldsymbol{X}(\boldsymbol{t}) \neq 0$, $\dot{\boldsymbol{V}} < 0$, and the asymptotic stability for the system is guaranteed [20].

Substituting equations (32)-(33) into (39), we obtained inequality for the V-time derivative as

$$\dot{\boldsymbol{V}} = \dot{\boldsymbol{e}}^T\boldsymbol{Q}\boldsymbol{e} + \boldsymbol{e}^T\boldsymbol{Q}\dot{\boldsymbol{e}} + \dot{\boldsymbol{X}}^T\boldsymbol{P}\boldsymbol{X} + \boldsymbol{X}^T\boldsymbol{P}\dot{\boldsymbol{X}} < 0 \tag{40}$$

Using the Equations (27), (28), (32), (33), (40) and **Lemma 1**, the results are got as follows

$$\dot{\boldsymbol{V}} = \begin{bmatrix} \boldsymbol{X}^T & \boldsymbol{e}^T \end{bmatrix} \begin{bmatrix} \boldsymbol{\theta} & 0 \\ 0 & \boldsymbol{J} \end{bmatrix} \begin{bmatrix} \boldsymbol{X} \\ \boldsymbol{e} \end{bmatrix} < \boldsymbol{0} \tag{41}$$

where,

$$\begin{aligned} \boldsymbol{\theta} = {} & \boldsymbol{P}(\boldsymbol{A} - \boldsymbol{B}\boldsymbol{K}^a) + (\boldsymbol{A} - \boldsymbol{B}\boldsymbol{K}^a)^T\boldsymbol{P} + \boldsymbol{P}((\varepsilon_3+\varepsilon_5)\boldsymbol{M}\boldsymbol{M}^T + \varepsilon_4\boldsymbol{B}\boldsymbol{B}^T)\boldsymbol{P} \\ & + (\varepsilon_3^{-1} + \varepsilon_5^{-1})(\boldsymbol{E}_1 - \boldsymbol{E}_2\boldsymbol{K}^a)^T(\boldsymbol{E}_1 - \boldsymbol{E}_2\boldsymbol{K}^a) < 0 \end{aligned} \tag{42}$$

$$\begin{aligned} \boldsymbol{J} = {} & \boldsymbol{Q}(\boldsymbol{A} - \boldsymbol{L}\boldsymbol{C}) + (\boldsymbol{A} - \boldsymbol{L}\boldsymbol{C})^T\boldsymbol{Q} + \boldsymbol{Q}(\varepsilon_1+\varepsilon_2)\boldsymbol{M}\boldsymbol{M}^T\boldsymbol{Q} \\ & + (\varepsilon_1^{-1} + \varepsilon_5^{-1})\boldsymbol{K}^{aT}\boldsymbol{E}_2^T\boldsymbol{E}_2\boldsymbol{K}^a + \varepsilon_4^{-1}\boldsymbol{K}^{aT}\boldsymbol{K}^a < 0 \end{aligned} \tag{43}$$

Pre and post Multiplication of Equation (42) with $\boldsymbol{P}^{-1}$ and use $\boldsymbol{N} = \boldsymbol{K}^a\boldsymbol{P}^{-1}$ and Schur complement, inequality (42) is described as follows

$$\begin{bmatrix} \boldsymbol{M}_1 & \boldsymbol{M}_2 & \boldsymbol{M}_3 \\ \boldsymbol{M}_2^T & (-\frac{1}{\varepsilon_3+\varepsilon_5})\boldsymbol{I} & 0 \\ \boldsymbol{M}_3^T & 0 & (-\frac{1}{\varepsilon_3^{-1}+\varepsilon_2^{-1}})\boldsymbol{I} \end{bmatrix} < 0$$

where, $\boldsymbol{M}_1 = \boldsymbol{A}\boldsymbol{P}^{-1} + \boldsymbol{P}^{-1}\boldsymbol{A}^T - \boldsymbol{B}\boldsymbol{N} - \boldsymbol{N}^T\boldsymbol{B}^T + \varepsilon_4\boldsymbol{B}\boldsymbol{B}^T$, $\boldsymbol{M}_2 = \boldsymbol{M}$, $\boldsymbol{M}_3 = \boldsymbol{P}^{-1}\boldsymbol{E}_1^T - \boldsymbol{N}^T\boldsymbol{E}_2^T$.

In the same way, we can obtained the result as follows

$$\begin{bmatrix} \boldsymbol{N}_1 & \boldsymbol{N}_2 & \boldsymbol{N}_3 \\ \boldsymbol{N}_2^T & -(\varepsilon_1+\varepsilon_2)^{-1}\boldsymbol{I} & 0 \\ \boldsymbol{N}_3^T & 0 & (-\dfrac{1}{\varepsilon_1^{-1}+\varepsilon_5^{-1}})\boldsymbol{I} \end{bmatrix} < 0$$

where, $\boldsymbol{T} = \boldsymbol{Q}\boldsymbol{L}$, $N_1 = \boldsymbol{Q}\boldsymbol{A} + \boldsymbol{A}^T\boldsymbol{Q} - \boldsymbol{T}\boldsymbol{C} - \boldsymbol{C}^T\boldsymbol{T}^T + \varepsilon_4^{-1}\boldsymbol{K}^{aT}\boldsymbol{K}^a$, $N_2 = \boldsymbol{Q}\boldsymbol{M}$, $N_3 = \boldsymbol{K}^{aT}\boldsymbol{E}_2^T$.
This completes the proof.

5. Numerical results

5.1. Analysis of free vibration for piezoelectric laminated composite rectangular cantilever plate

In this section, the dynamic behaviour of piezoelectric laminated composite rectangular cantilever plate is described. The width and thickness are $b = 1\text{m}$ and $h = 5\text{mm}$ for the composite laminate. The thickness of actuator and sensor is $t_p = 2\text{mm}$. The free vibration of the composite laminate with piezoelectric actuator and sensor in hygrothermal environment is calculated.

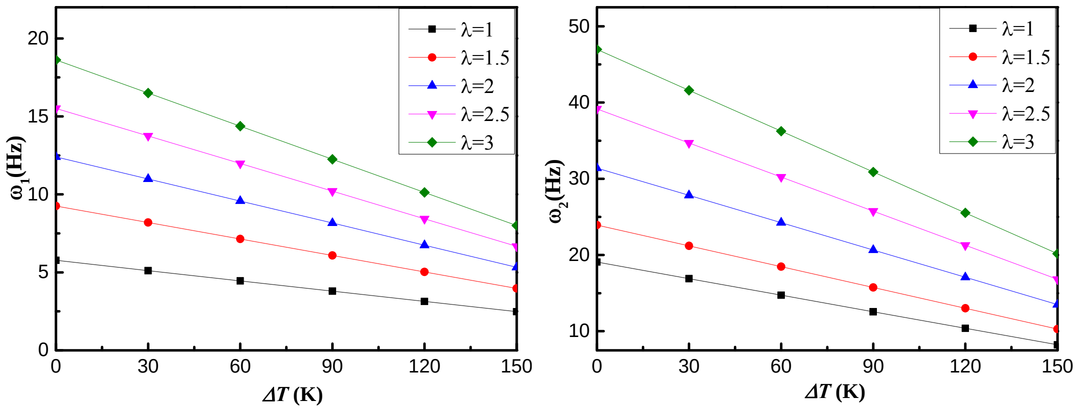

Figure 2. (a)-(b): The influence of temperature (ΔT(k)) on the vibrational natural frequencies of laminated rectangular cantilever composite plate with K=5

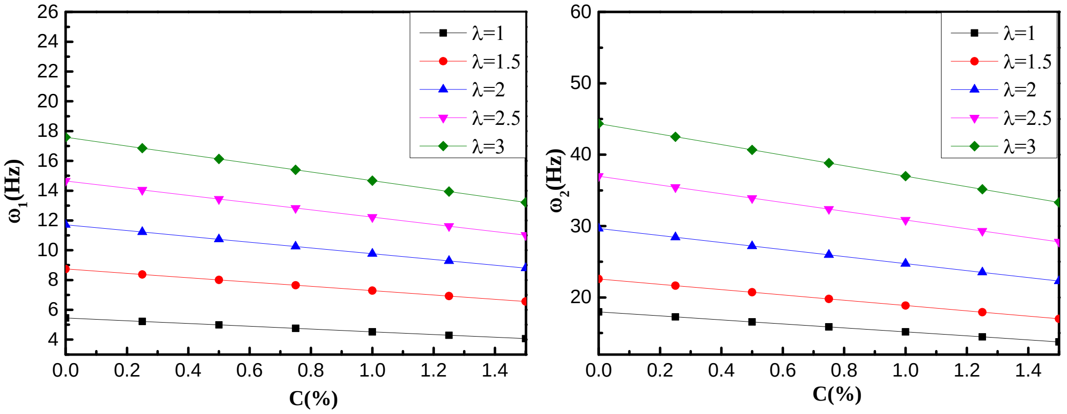

Figure 3. (a)-(b): The influence of moisture (C) on the vibrational natural frequencies of laminated rectangular cantilever composite plate with K=5

Figure 2 and Figure 3 show the influence of temperature rise (ΔT) and moisture concentration rise (C) on the dimensionless natural frequencies under five different dimensionless aspect ratio λ. It can be seen from these figures that the rises of temperature and humidity concentration lead to a decrease of the first-order and second-order natural frequency. Also, the temperature has a greater effect on frequency than moisture, as shown in Figure 2. The result is consistent with the paper from Ram et.al [6] who used the finite element formulation to calculate the dynamic behaviour of various boundary conditions for laminated composite plate subjected to hygrothermal loading. Further, when $b = 1\text{m}$, the first-order and second-order natural frequency increase with the increase in aspect ratio λ. Also, the variations are approximately linear with the rises of temperature (ΔT) and moisture (C), as shown in Figure 2 and Figure 3.

5.2. Vibration Suppression Analysis of the Piezoelectric Composite Rectangular Cantilever Plate

To verify the efficiency analysis and accuracy of robust controller, the mechanical model of instance is given in figure 1, here, the thickness of piezoelectric patches and host plate is $t_p = 2\text{mm}$ and $h = 5\text{mm}$ respectively. We assume

$$\varepsilon_1 = \varepsilon_2 = \varepsilon_3 = \varepsilon_4 = \varepsilon_5 = 1 \tag{44}$$

$$\boldsymbol{E}_1 = \begin{bmatrix} 1 & 0 & 0 & 0 \\ 0 & 1 & 0 & 0 \\ 0 & 0 & 1 & 0 \\ 0 & 0 & 0 & 1 \end{bmatrix}, \ \boldsymbol{E}_2 = \begin{bmatrix} 0.1 \\ 0.2 \\ 0.2 \\ 0.1 \end{bmatrix}, \ \boldsymbol{M} = \begin{bmatrix} 1 & 0 & 0 & 0 \\ 0 & 1 & 0 & 0 \\ 0 & 0 & 1 & 0 \\ 0 & 0 & 0 & 1 \end{bmatrix} \tag{45}$$

Using equation (44) and (45) and the **Theorem 1**, the feedback gain matrix is as follows

$$\boldsymbol{K} = \begin{bmatrix} -0.52441 & -9.16542 & 7.39912 & 18.80072 \end{bmatrix} \tag{46}$$

The uncontrolled and controlled time history curves of the laminated composite rectangular cantilever plate with piezoelectric sensors and actuators are shown in Figure 4. It is seen from these figures that the first-order and second-order transversal displacements is suppressed to be convergent after the control strategy is applied.

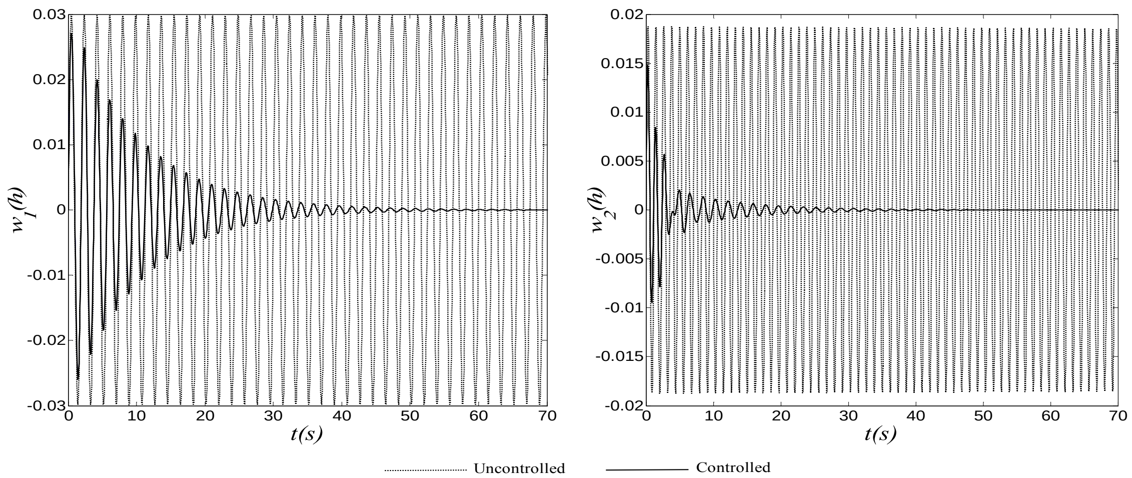

Figure 4. Uncontrolled and controlled first-order and second-order time history curves of the laminated composite rectangular cantilever plate with the initial temperature and moisture change is $\Delta T = 25\text{K}$ and C=0.25 respectively.

Considering the change of the temperature (ΔT) and moisture concentration (C), the uncontrolled and controlled first-order and second-order time history curves of the plate are simulated, the results are shown in Figure 5 and Figure 6.The results illustrate that the control strategy have a good suppression for the free vibrational behaviour of the laminated composite rectangular cantilever plate under different hygrothermal environment. Thus, the results show that the present vibration control method is effective and accurate.

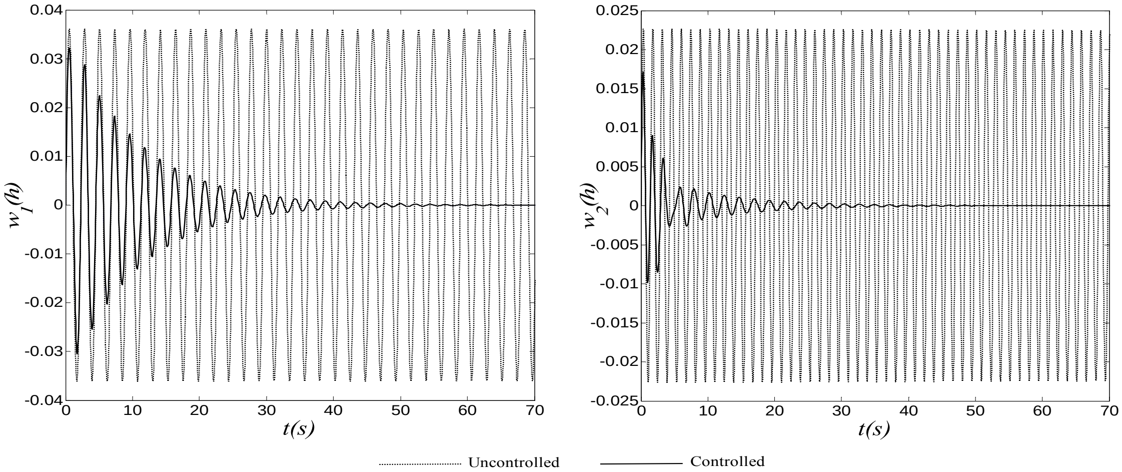

Figure 5. Uncontrolled and controlled first-order and second-order time history curves of the laminated composite rectangular cantilever plate with the initial temperature and moisture change is $\Delta T = 100\text{K}$ and C=0.25 respectively.

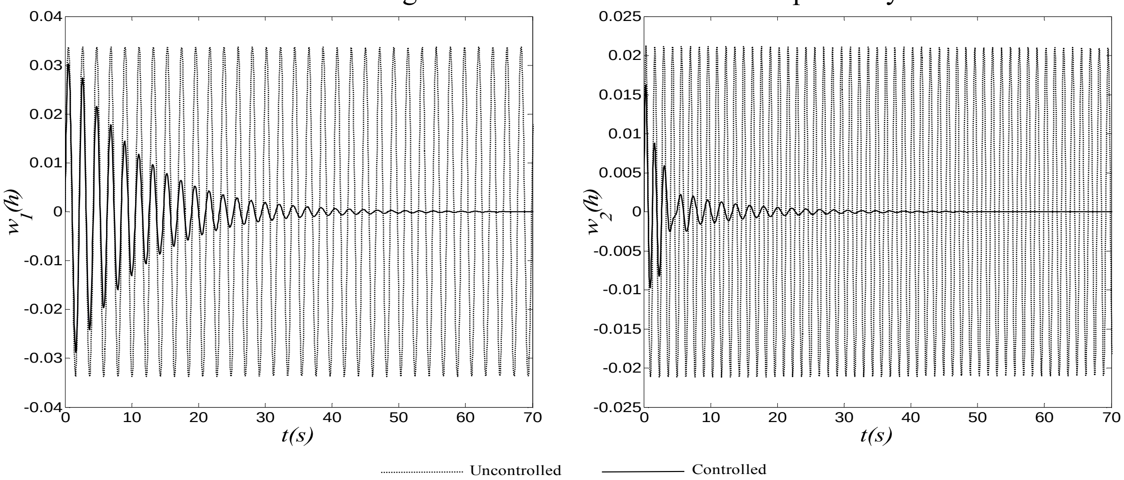

Figure 6. Uncontrolled and controlled first-order and second-order time history curves of the laminated composite rectangular cantilever plate with the initial temperature and moisture change is $\Delta T = 25\text{K}$ and C=1.5 respectively.

6. Conclusions

In this paper, the vibration suppression for a cantilevered rectangular piezoelectric laminated composite plate subjected to the hygrothermal loading is proposed by using the piezoelectric patches as the actuators and sensors, respectively. The conclusions are as follows:

(1) The dynamics equation is derived based on Hamilton's principle. The partial differential equations are discretized through Galerkin method. Based on the state space equation, the output feedback controller is designed. Constructing full-dimensional state observer, the estimated state feedback is introduced to construct a closed-loop feedback system.

(2) By numerical simulation, we can find that the reduction of first-order and second-order natural frequency with the increase of temperature and moisture. Further, the accuracy and efficiency of the controller in supressing the free vibrations of the cantilevered rectangular piezoelectric

laminated composite plate under the different hygrothermal environment are shown by the numerical examples.

7. References

[1] Tatiane C D G, Trindade M A 2011 Modeling and analysis of laminate composite plates with embedded active-passive piezoelectric networks *J. Sound Vib*. 330 p194-216
[2] Cook A C, Vel S S 2012 Multiscale analysis of laminated plates with integrated piezoelectric fiber composite actuators *Compos. Struct.* 94 p 322-336
[3] Leung A Y T, Zheng J J, Lim C W et al 2008 A new symplectic approach for piezoelectric cantilever composite plates *Compos. Struct.* 86 p 1865-1874
[4] Zhang Y F, Zhang W, Yao Z G 2018 Analysis on nonlinear vibrations near internal resonances of a composite laminated piezoelectric rectangular plate *Eng. Struct*. 173 p 89-106
[5] Sreehari V M, Maiti D K 2015 Buckling and post buckling analysis of laminated composite plates in hygrothermal environment using an inverse hyperbolic shear deformation theory *Compos. Struct.*129 p 250-255
[6] Ram S K S, Sinha P K 1992 Hygrothermal effects on the free vibration of laminated composite plates*J. Sound Vib.* 158 p 133-148
[7] Radić N, Jeremić D 2017 A comprehensive study on vibration and buckling of orthotropic double-layered graphene sheets under hygrothermal loading with different boundary conditions *Compos. Part B-Eng* 128 p 182-199
[8] Malekzadeh P and BeniA A 2010 Free vibration of functionally graded arbitrary straight-sided quadrilateral plates in thermal environment *Compos. Struct.*92 p 2758-2767
[9] Mahapatra T R and Panda S K 2016 Nonlinear free vibration analysis of laminated composite spherical shell panel under elevated hygrothermal environment: A micromechanical approach. *Aerosp. Sci.Technol.*49 p 276-288
[10] Rath M K and Sahu S K 2012 Vibration of woven fiber laminated composite plates in hygrothermal environment*J. Vib. Control* 18 p 1957-1970
[11] Shenas A G and Malekzadeh P 2016 Free vibration of functionally graded quadrilateral microplates in thermal environment *Thin Wall Struct.* 106 p 294-315
[12] Ye T, Jin G, Gao S 2018 Three-dimensional hygrothermal vibration of multi-layered cylindrical shells *Compos.Struct.* 201 p 867-881
[13] Phung Van P, Nguyenthoi T, Ledinh T and Nguyenxuan H 2013 Static and free vibration analyses and dynamic control of composite plates integrated with piezoelectric sensors and actuators by the cell-based smoothed discrete shear gap method (cs-fem-dsg3)*SmartMater. Struct.*22, 095026
[14] He X Q, Ng, T Y, Sivashanker S andLiew K M 2001 Active control of FGM plates with integrated piezoelectric sensors and actuatorsInt.*J. Solids Struct.*38 p 1641-1655
[15] Song Z. G, Zhang L W and Liew K M 2016 Active vibration control of CNT reinforced functionally graded plates based on a higher-order shear deformation theory *Int. J.Mech. Sci.*105 p 90-101
[16] Zhang W, Zhao M H and Guo X Y 2013 Nonlinear responses of a symmetric cross-ply composite laminated cantilever rectangular plate under in-plane and moment excitations. *Compos. Struct.*100 p 554-565
[17] Liu Q and Paavola J 2016 General analytical sensitivity analysis of composite laminated plates and shells for classical and first-order shear deformation theories *Compos. Struct.*183 p 21-34
[18] Shen H S, Zheng J J and Huang X L 2004 The effects of hygrothermal conditions on the dynamic response of shear deformable laminated plates resting on elastic foundations *J. Reinf. Plast Comp.* 23 p 1095-1113
[19] Thai H T and Choi D H 2013 A simple first-order shear deformation theory for laminated composite plates *Compos. Struct.* 106 p 754-763

[20] Nader J 2010 Piezoelectric-based vibration control from macro to micro/nanoscale systems (Springer US)
[21] Cook R D, Malkus D S and Plesha M E 2000 Concepts and Applications of Finite Element Analysis third edition (New York: John Wiley &Sons)
[22] Zhang W and Zhao M H 2012 Nonlinear vibrations of a composite laminated cantilever rectangular plate with one-to-one internal resonance *Nonlinear Dynam.* 70 p 295-313
[23] Reddy J N 2004 Mechanics of laminated composite plates and shells: Theory and Analysis (Boca Raton :CRC Press LLC)
[24] Sulbhewar L N and Raveendranath P 2016 A timoshenko piezoelectric beam finite element with consistent performance irrespective of geometric and material configurations *Lat. Am. J. Solids Stru.* 13 p 992-1015
[25] Huang X L and Shen H S 2006 Vibration and dynamic response of functionally graded plates with piezoelectric actuators in thermal environments *J. SoundVib.*289 p 25-53
[26] Wang Z and Unbehauen H 2000 A class of nonlinear observers for discrete-time systems with parametric uncertainty *Int. J. Syst. Sci.* 31 p 19-26

Acknowledgments
The authors sincerely acknowledge the financial support of the National Natural Science Foundation of China (NNSFC) through Grant No. 11862020, No. 11502122, No. 11402126, and Inner Mongolia Natural Science Foundation (No. 2018LH01014).